www.ietdl.org

Published in IET Systems Biology
Received on 19th August 2013
Revised on 10th December 2013
Accepted on 11th December 2013
doi: 10.1049/iet-syb.2013.0021

ISSN 1751-8849

Dynamic flux balance analysis for synthetic microbial communities

Michael A. Henson, Timothy J. Hanly

Department of Chemical Engineering, University of Massachusetts, Amherst, MA 01007, USA
E-mail: henson@ecs.umass.edu

Abstract: Dynamic flux balance analysis (DFBA) is an extension of classical flux balance analysis that allows the dynamic effects of the extracellular environment on microbial metabolism to be predicted and optimised. Recently this computational framework has been extended to microbial communities for which the individual species are known and genome-scale metabolic reconstructions are available. In this review, the authors provide an overview of the emerging DFBA approach with a focus on two case studies involving the conversion of mixed hexose/pentose sugar mixtures by synthetic microbial co-culture systems. These case studies illustrate the key requirements of the DFBA approach, including the incorporation of individual species metabolic reconstructions, formulation of extracellular mass balances, identification of substrate uptake kinetics, numerical solution of the coupled linear program/differential equations and model adaptation for common, suboptimal growth conditions and identified species interactions. The review concludes with a summary of progress to date and possible directions for future research.

1 Introduction

1.1 Metabolic flux balance analysis (FBA)

Metabolic FBA is based on stoichiometric cell models that mathematically represent the biochemical reactions in a metabolic network. The essential information required to construct a stoichiometric model is a list of participating biochemical species (metabolites), a list of the relevant intracellular reactions involving these species, and the stoichiometric coefficients for every species in each reaction [1, 2]. Each intracellular metabolite is assumed to exhibit negligible accumulation such that the fluxes producing the metabolite are balanced by the fluxes consuming the metabolite. Steady-state mass balances on the intracellular metabolites can be gathered to form a matrix equation of the form

$$\boldsymbol{A}\boldsymbol{v} = \boldsymbol{0} \tag{1}$$

where $\boldsymbol{A}$ is the stoichiometric matrix with m rows corresponding to the number of balanced metabolites and n columns corresponding to the number of fluxes. The matrix entry a_{ij} is the stoichiometry of the ith species participating in the jth reaction.

The objective of FBA is to solve (1) for the fluxes $\boldsymbol{v}$. Given lower and upper bounds on the fluxes and the substrate uptake rates, intracellular and secretion fluxes are calculated. For most stoichiometric models of practical interest, the metabolic network contains more unknown fluxes than the balanced intracellular species, and the linear system (1) is underdetermined. Typically the fluxes are resolved by solving a linear program (LP) formulated under the assumption that the cell utilises available resources to maximise growth [3, 4]. The growth rate μ is calculated as the weighted sum of the fluxes contributing to biomass formation. Fluxes corresponding to biomass precursors (amino acids, carbohydrates, ribonucleotides, deoxyribonucleotides, lipids, sterols, phospholipids, fatty acids etc.) are assigned weights w_i according to their contribution to biomass and the remaining fluxes are given weights of zero, such that $\mu = \boldsymbol{w}^{\mathrm{T}}\boldsymbol{v}$ [5]. The LP to be solved has the form

$$\begin{aligned} \max_{\boldsymbol{v}} \ & \mu = \boldsymbol{w}^{\mathrm{T}}\boldsymbol{v} \\ & \boldsymbol{A}\boldsymbol{v} = \boldsymbol{0} \\ & \boldsymbol{v}_{\min} \le \boldsymbol{v} \le \boldsymbol{v}_{\max} \end{aligned} \tag{2}$$

where $\boldsymbol{v}_{\min}$ and $\boldsymbol{v}_{\max}$ are the vectors containing lower and upper bounds on the fluxes, respectively. The FBA problem (2) can be efficiently and reliably solved by a variety of LP solvers.

Stoichiometric cell models have been constructed for organisms ranging in complexity from bacteria to mammals. With the advent of sequencing technology, genome-scale stoichiometric models that account for all known gene–protein-reaction associations have been developed for many organisms [5]. These genome-scale reconstructions have been used extensively for predicting cellular growth and product secretion patterns in microbial systems [4, 6, 7]. Extensions of classical FBA allow the redesign of metabolic networks for the overproduction of desired metabolites through gene deletions and insertions, which

are implemented by removing or adding intracellular reactions to produce a network of the engineered mutant [8–10]. An alternative method called minimisation of metabolic adjustment (MOMA) that is based on minimising the least-squares difference between the wild-type and mutant fluxes has been argued to provide more accurate mutant flux predictions [11]. These computational methods provide metabolic engineering targets that are experimentally testable. A wide variety of FBA-related analysis methods are available in software tools such as the constraint-based reconstruction and analysis (COBRA) toolbox that runs in the MATLAB environment [12].

1.2 Motivation for dynamic modelling

Classical FBA allows prediction of cellular growth and product secretion rates for fixed values of the substrate uptake rates. As a result, FBA is strictly applicable only to the balanced growth phase in batch cultures and the steady-state growth in continuous cultures. Dynamic FBA (DFBA) is an extension of classical FBA that accounts for cell culture dynamics and allows prediction of cellular metabolism in batch and fed-batch fermentations [13–15]. The basic DFBA framework is depicted in Fig. 1 for the case of batch culture. The growth rate μ, the intracellular fluxes $\boldsymbol{v}$ and the product secretion rates $\boldsymbol{v}_p$ are computed through solution of the classical FBA problem (2). Rather than specifying constant substrate uptake rates, extracellular substrate concentrations $\boldsymbol{S}$ and product concentrations $\boldsymbol{P}$ are used for calculation of time-varying substrate uptake rates $\boldsymbol{v}_s$ through expressions for the uptake kinetics. The calculation of time-varying uptake rates allows metabolism to change dramatically, as observed with substrate limitation and eventually exhaustion during batch culture. These substrate uptake rates represent maximum rates possible because of transport limitations and are incorporated as upper bounds on the calculated uptake rates. The extracellular concentrations are computed by solving extracellular balance equations for the biomass concentration X and the substrate and product concentrations given growth and secretion rates obtained from the LP. Although the cell is assumed to maintain an intracellular steady state, all the intracellular and extracellular variables are time varying.

DFBA is particularly attractive because the increasing availability of flux balance models is fully leveraged and very little additional information is required for model construction. As discussed in Section 2, the principal challenges associated with DFBA are experimental determination of the substrate uptake kinetics and numerical solution of the dynamic model. DFBA offers important

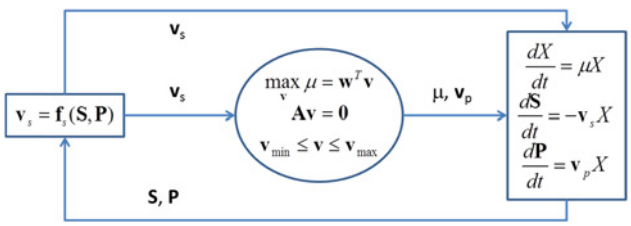

Fig. 1 *Dynamic flux balance model for growth of a single microbial species in a batch culture with substrate concentrations* $\boldsymbol{S}(t)$*, product concentrations* $\boldsymbol{P}(t)$ *and biomass concentration* $X(t)$*. Here,* $\boldsymbol{v}_s(t)$ *is the subset of fluxes for substrate uptakes,* $\boldsymbol{v}_p(t)$ *is the subset of fluxes for product secretion rates and* $\boldsymbol{f}_s(\boldsymbol{S}, \boldsymbol{P})$ *is a vector function of substrate uptake kinetics.*

advantages over alternative transient modelling frameworks. As simple unstructured models rely on phenomenological descriptions of cell growth and constant yield coefficients [16], they have limited predictive capability and cannot describe genetic alterations. Although alternative dynamic modelling approaches such as structured kinetic models [17, 18] log-linear kinetic models [19] and cybernetic models [20, 21] hold considerable promise, their application is often limited by need for *in vivo* enzyme kinetics. DBFA provides a practical alternative for incorporating intracellular structure. Given the availability of a classical flux balance model, only a small number of additional parameters are needed to account for the substrate uptake kinetics. A well-documented weakness of the flux balance approach is the difficulty associated with incorporating cellular regulation. This problem has been partially addressed in FBA by using gene expression data to constrain regulated fluxes within the metabolic network [22–24]. Furthermore, DFBA offers the possibility of formulating substrate uptake kinetics to account for known regulatory processes as shown in Section 3.

1.3 Application to synthetic microbial communities

Biotechnology research has traditionally focused on individual microbial strains that are perceived to have the necessary metabolic functions, or the capability to have these functions introduced, to achieve a particular task. For many important applications, the development of such omni-potent microbes is an extremely challenging if not impossible problem. By contrast, nature employs a radically different strategy based on synergistic combinations of different microbial species that collectively achieve the desired task [25, 26]. These natural communities have evolved to exploit the native metabolic capabilities of each species and are highly adaptive to changes in their environments. Until recently, microbial communities were difficult to study because of a lack of suitable experimental and computational tools. With the advent of high-throughput genome sequencing, omics technologies and bioinformatics, researchers now have unprecedented capabilities to analyse and engineer the metabolism of microbial communities.

Genome sequencing of whole communities in natural environments (metagenomics) is now possible [27, 28], and a wealth of sequence data have been generated for various communities [29–31]. Although genome sequencing can be valuable for initial exploration, in silico models of community metabolism can provide additional information on metabolic capabilities and the extent of metabolic interactions in microbial communities [32]. Extending genome-scale modelling approaches to natural microbial communities is challenging because of the difficulties associated with isolating individual members of the community, modelling the metabolism of multiple, poorly characterised species and capturing metabolic interactions between species, which can include competition, cross-feeding, syntrophy and mutualism. Therefore genome-scale modelling primarily has been applied to synthetic microbial communities comprised of a few, well characterised microbes. Both steady-state [33–36] and dynamic [37–43] FBA methods have been developed and applied to the analysis and design of community metabolism. Despite these recent advances, generally

applicable in silico tools for microbial communities that parallel methods for single species are needed.

1.4 Scope of this review

The goal of this review is to illustrate the application of genome-scale modelling and flux balance analysis to microbial communities. Synthetic rather than natural communities are emphasised because of their superior tractability with respect to the modelling of individual species metabolism and species interactions [25, 44]. Furthermore, dynamic rather than classical FBA is emphasised since this approach offers an increased capability for capturing time-varying species metabolism and interactions. Readers interested in the application of classical FBA to microbial communities are referred to another recent review by Mahadevan and Henson [45]. As the dynamic flux balance modelling of microbial communities is an emerging area, Section 2 is focused on describing the key elements involved in model development including the incorporation of individual species metabolic models, formulation of extracellular mass balances, identification of substrate uptake kinetics, numerical solution of the coupled linear program/differential equations and model adaptation for community growth conditions and identified species interactions. Section 3 contains two biofuel-related problems studied by the authors: (i) simultaneous glucose and xylose consumption by *Saccharomyces cerevisiae* (*S. cerevisiae*)/*Escherichia coli* (*E. coli*) co-cultures [40]; and (ii) detoxification of biomass hydrolysates by *S. cerevisiae*/*Scheffersomyces stipitis* (*S. stipitis*) co-cultures [41]. The paper is concluded with a discussion of major accomplishments and future research needs for dynamic flux balance modelling of microbial communities.

2 Dynamic FBA

2.1 Intracellular flux balance model

A prerequisite for DFBA of a synthetic microbial community is the availability or development of a metabolic network model for each species in the community. Typically genome-scale metabolic reconstructions are used for this purpose because of their known gene–protein–reaction associations and superior predictive capability compared with smaller scale reconstructions [13]. Given the ever expanding database of genome-scale reconstructions, an advantage of applying DFBA to synthetic communities comprised a small number of well characterised species is that the necessary reconstructions are often available. Otherwise, genome-scale reconstructions must be developed for the unmodelled species [38]. Until recently, manual curation has been the only alternative for metabolic network reconstruction [5]. However, computational pipelines such as the Model SEED [46], Pathway Tools [47] and MicrobesFlux [48] are now available for automated generation of draft metabolic models. The Model SEED currently contains over 3000 publically available genome-scale models, and a draft model can be generated for any organism for which an annotated genome is available on the SEED platform [49]. However, such draft models invariably require some degree of manual curation to improve their network fidelity and predictive capability.

Assuming the necessary genome-scale reconstructions are available, the stoichiometric model for each species has the form

$$\boldsymbol{A}_i\boldsymbol{v}_i = \boldsymbol{0} \quad \boldsymbol{v}_{i,\min} \le \boldsymbol{v} \le \boldsymbol{v}_{i,\max} \tag{3}$$

where $\boldsymbol{A}_i$ is the stoichiometric matrix, $\boldsymbol{v}_i$ is the flux vector and $\boldsymbol{v}_{i,\min}$ and $\boldsymbol{v}_{i,\max}$ are the minimum and maximum flux vectors associated with the ith species. A composite stoichiometric network model for n species can be constructed as follows

$$\begin{bmatrix} \boldsymbol{A}_1 & \boldsymbol{0} & \boldsymbol{0} & \boldsymbol{0} \\ \boldsymbol{0} & \boldsymbol{A}_2 & \boldsymbol{0} & \boldsymbol{0} \\ \boldsymbol{0} & \boldsymbol{0} & \ddots & \boldsymbol{0} \\ \boldsymbol{0} & \boldsymbol{0} & \boldsymbol{0} & \boldsymbol{A}_n \end{bmatrix} \begin{bmatrix} \boldsymbol{v}_1 \\ \boldsymbol{v}_2 \\ \vdots \\ \boldsymbol{v}_n \end{bmatrix} = \begin{bmatrix} \boldsymbol{0} \\ \boldsymbol{0} \\ \vdots \\ \boldsymbol{0} \end{bmatrix} \Rightarrow \boldsymbol{A}\boldsymbol{v} = \boldsymbol{0}$$

$$\begin{bmatrix} \boldsymbol{v}_{1,\min} \\ \boldsymbol{v}_{2,\min} \\ \vdots \\ \boldsymbol{v}_{n,\min} \end{bmatrix} \le \begin{bmatrix} \boldsymbol{v}_1 \\ \boldsymbol{v}_2 \\ \vdots \\ \boldsymbol{v}_n \end{bmatrix} \le \begin{bmatrix} \boldsymbol{v}_{1,\max} \\ \boldsymbol{v}_{2,\max} \\ \vdots \\ \boldsymbol{v}_{n,\max} \end{bmatrix} \Rightarrow \boldsymbol{v}_{\min} \le \boldsymbol{v} \le \boldsymbol{v}_{\max} \tag{4}$$

By analogy to compartmentalised models for eukaryotic organisms such as yeasts [50], this formulation can be viewed as assigning each species to a separate compartment and assuming that no direct exchange of metabolites occurs between these compartments. Instead, metabolites are assumed to be exchanged in a time-varying manner through a separate extracellular compartment (see Section 2.2). This feature is a distinct advantage of DFBA compared with proposed extensions of classical FBA [34, 35], which require that metabolite exchange rates are constant and do not allow transient prediction of exchanged metabolite concentrations. If the individual species models include separate compartments for distinct cellular organelles, then the model will be comprised intraspecies compartments that exchange metabolites, interspecies compartments that do not exchange metabolites and the extracellular compartment.

As in the single-species case, FBA for microbial communities involves solving (4) for the fluxes $\boldsymbol{v}$ given values of substrate uptake fluxes. As the metabolic network of each species is invariably undetermined with more unknown fluxes than balanced species, the fluxes of the community are usually resolved through solution of a suitably posed optimisation problem. Unlike the single-species case (2) where growth rate maximisation is usually perceived as a suitable cellular objective [2], specification of a meaningful objective for microbial communities is more challenging because of complex trade-offs between individual- and community-level fitness requirements. The OptCom computational framework [51] was developed to provide considerable flexibility with respect to the community model objective by allowing the incorporation of species-level fitness criteria as well as community-level optimisation. In the absence of specific information about individual species objectives, a reasonable approach is to assume that the community attempts to maximise its total growth rate [37]. This assumption leads to the following LP problem that is the multispecies extension of (2)

$$\begin{aligned} \max_{\mathrm{v}} \ & \mu = \mu_1 + \mu_2 + \cdots + \mu_n = \boldsymbol{w}^{\mathrm{T}}\boldsymbol{v} \\ & \boldsymbol{A}\boldsymbol{v} = \boldsymbol{0} \\ & \boldsymbol{v}_{\min} \le \boldsymbol{v} \le \boldsymbol{v}_{\max} \end{aligned} \tag{5}$$

doi: 10.1049/iet-syb.2013.0021

where the stoichiometric matrix $\boldsymbol{A}$ and flux vectors $\boldsymbol{v}$, $\boldsymbol{v}_{\min}$ and $\boldsymbol{v}_{\max}$ are defined in (4) and $\boldsymbol{w}$ is a partitioned vector of biomass weighing coefficients containing the coefficients of the individual species. Classical FBA is extended to the community model by specifying substrate uptake fluxes of the individual species and solving (5) for the unknown fluxes. Species interactions can be modelled through metabolite exchange assuming that the total production rate of each secreted metabolite is equal to the total uptake rate of that metabolite by other species [35]. By contrast, the DFBA approach allows secreted metabolites to accumulate and affect the uptake rates of the supplied substrates and other exchanged metabolites. As explained below, these uptake rates are posed as constraints in the DFBA problem to account for species interactions.

2.2 Extracellular dynamic model

When applied to community models, classical FBA is even more limited than in the single-species case because the additional assumption that metabolite exchange rates are constant must be invoked. As the accumulation of extracellular metabolites is not allowed within the FBA framework, this assumption implies that metabolites must be consumed by community members at the same rate that they are produced by other community members [34, 35]. The steady-state assumption inherent in classical FBA can be removed by extending DFBA to multiple species as shown in Fig. 2 [37]. The growth rate μ_i, intracellular fluxes $\boldsymbol{v}_i$ and the product secretion fluxes $\boldsymbol{v}_{\mathrm{p},i}$ of each species i are computed through solution of the FBA problem (5). Extracellular mass balances are included for all consumed substrates and secreted products that are believed to influence community metabolism. These dynamic balances are numerically integrated to determine the biomass concentrations X_i, the substrate concentrations $\boldsymbol{S}$ and the product concentrations $\boldsymbol{P}$ given growth rates and metabolite secretion fluxes of individual species obtained from the LP. If species i does not consume a particular substrate, then the element of $\boldsymbol{v}_{\mathrm{s},i}$ associated with that substrate will be zero. Similarly, if species i does not synthesise a particular product, then the element of $\boldsymbol{v}_{\mathrm{p},i}$ associated with that product will be zero. Although not shown in Fig. 2, the model may also include extracellular mass balances on gaseous substrates such as oxygen that affect growth and gaseous products such as carbon dioxide that are readily measured for model validation. In particular, gas and liquid phase oxygen balances are often required to satisfactorily predict the dissolved oxygen concentration under partially aerobic or microaerobic growth conditions in aerated bioreactors [41].

The extracellular substrate concentrations $\boldsymbol{S}$ and product concentrations $\boldsymbol{P}$ are used for calculation of time-varying substrate consumption rates $\boldsymbol{v}_{\mathrm{s}}$ through expressions for the uptake kinetics. These substrate uptake rates represent maximum rates possible because of transport limitations and are incorporated as upper bounds on the uptake rates calculated in the FBA problem. Assuming the maximum growth rate objective in (5) is valid, the primary challenge associated with developing a dynamic flux balance model is identification of appropriate uptake kinetics between each substrate/species pair. If species i is known not to consume a particular substrate, then the element of $\boldsymbol{v}_{\mathrm{s},i}$ associated with that substrate can be set to zero. Typically Michaelis–Menten-type expressions with additional terms for inhibition effects are used to model substrate uptake kinetics [40]. As compared with classical FBA, an important advantage of DFBA is that complex regulatory mechanisms such as diauxic consumption of substrates and growth inhibition by extracellular metabolites can be included in a phenomenological manner through the uptake expressions [37]. Commonly used uptake expressions include

$$
\begin{aligned}
v_{\mathrm{s}j} &= \frac{v_{\mathrm{m}} S_j}{K_{\mathrm{m}} + S_j} \\
v_{\mathrm{s}j} &= \frac{v_{\mathrm{m}} S_j}{K_{\mathrm{m}} + S_j} \frac{1}{1 + S_k / K_{\mathrm{s}}} \\
v_{\mathrm{s}j} &= \frac{v_{\mathrm{m}} S_j}{K_{\mathrm{m}} + S_j} \frac{1}{1 + P_k / K_{\mathrm{p}}}
\end{aligned}
\tag{6}
$$

where S_j and S_k are the concentration of substrates j and k, respectively, P_k is the concentration of product k, v_{m} and K_{m} are the Michaelis–Menten constants and K_{s} and K_{p} are the inhibition constants. The first equation describes purely substrate-limited uptake, the second equation describes uptake inhibition by a preferred substrate and the third equation describes uptake inhibition by a secreted product. The third equation allows the modelling of species interactions where a metabolic by-product secreted by one species inhibits the substrate uptake rate, and therefore the growth rate, of another species. Specification of appropriate uptake kinetics for each substrate/species pair is highly problem dependent and typically requires a combination of a priori knowledge and iterative modelling [40].

The DFBA problem depicted in Fig. 2 involves solution of a non-linear differential equation system with an embedded LP. Three general approaches have been proposed for numerical solution of dynamic flux balance models. The sequential approach involves time discretisation of the model equations such that the substrate uptake kinetics, the FBA LP and the extracellular balances can be solved separately and sequentially [14, 52, 53]. We have found this method to be computationally inefficient and prone to stability problems, especially as the size of the LP grows. As an alternative, we have developed a simultaneous solution approach in which the uptake kinetics and the LP are embedded within the extracellular equation solution such that explicit time discretisation is avoided and high-performance integration codes can be used directly [24, 37]. More recently, an efficient and reliable solution method was developed by reformulating the model as a differential-algebraic equation system [54]. This method offers the advantage that the embedded LP only has to be solved when the structure of the optimal flux distribution changes, which typically occurs infrequently as compared with the number of integration steps.

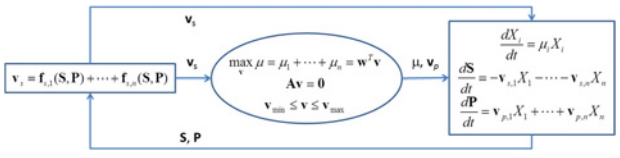

Fig. 2 *Dynamic flux balance model for growth of a microbial community in a batch culture with substrate concentrations* $\boldsymbol{S}(t)$*, product concentrations* $\boldsymbol{P}(t)$ *and biomass concentration* $X_i(t)$ *for the ith species. Here,* $\boldsymbol{v}_{s,\,i}(t)$ *are substrate uptake fluxes,* $\boldsymbol{v}_{p,\,i}(t)$ *are the product secretion fluxes and* $\boldsymbol{f}_{s,i}(\boldsymbol{S},\,\boldsymbol{P})$ *are substrate uptake functions for the* ith *species.*

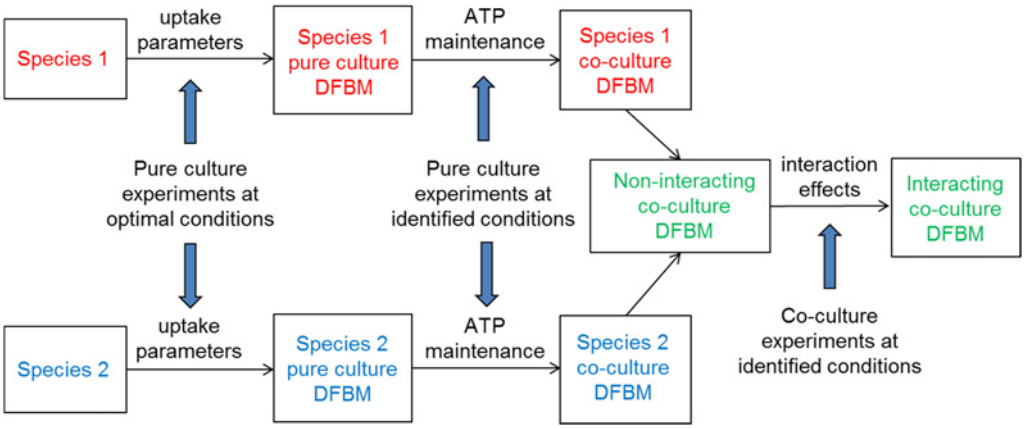

Fig. 3 *Integration of pure and co-culture fermentation experiments with DFBM to develop a predictive co-culture model that account for common growth conditions and species interactions*

2.3 Model development procedure

The previous two sections outline the mathematical foundations of DFBA for microbial communities. The development of a predictive model requires integration of fermentation experiments and dynamic simulations. In addition to pure culture experiments required to identify the substrate uptake kinetics for the individual species, co-culture experiments are needed to model the effects of: (i) common temperature and pH conditions that promote community growth when the individual species do not share the same optimal growth conditions; and (ii) unknown interactions between the various species that cannot be identified in pure culture. Fig. 3 shows the model development procedure we developed for co-culture systems [40]. Pure culture batch fermentation experiments are performed to determine the substrate uptake kinetics of each microbe at its optimal pH and temperature. These uptake kinetics are combined with genome-scale reconstructions of intracellular metabolism and dynamic extracellular mass balances to develop a pure culture dynamic model of each microbe for optimal growth on its respective substrates. Then a series of pure culture batch experiments are performed to determine a common pH and temperature that maximises the combined biomass productivity of the two microbes. As discussed in the following section, we have found that good predictions of pure culture dynamics at these suboptimal conditions can be obtained by increasing the non-growth associated ATP maintenance of each microbe. Finally, a series of co-culture experiments are performed at the identified co-culture conditions for different substrate mixtures to identify possible interactions between the two species. Cell concentration measurements of each species are required to develop and validate the dynamic model. If the two species differ significantly in cell size, then the individual cell concentrations can be determined by particle size distribution analysis (first case study in Section 3). Otherwise, individual cell counting using a hemacytometer may be required (second case study in Section 3).

In principle, the model development procedure shown in Fig. 3 can be scaled to multiple species, although considerably more work may be required. For example, a synthetic community consisting of three species could require as many as three sets of pure culture experiments to identify the substrate uptake rates of the individual species, two sets of co-culture experiments to identify the specific interactions between each of the two possible species pairs, and one set of three-species community experiments.

3 Case studies

3.1 Glucose and xylose consumption by *S. cerevisiae*/*E. coli* co-cultures

3.1.1 Strain selection: In this work [40], we focused on the problem of efficient glucose and xylose utilisation with a co-culture system comprised of wild-type *S. cerevisiae* and the engineered *E. coli* strain ZSC113. Our interest in this particular system was attributable to several factors. *S. cerevisiae* rapidly consumes glucose, whereas *E. coli* can natively metabolise pentose sugars such as xylose [55]. A stable mixed-culture of these two species has been developed for continuous fermentation [56]. Synergy has been observed in the fermentation of biomass hydrolysates, as *S. cerevisiae* can metabolise some compounds that are toxic to *E. coli* [57, 58]. Furthermore, both species have well-established genome-scale reconstructions [7, 59] for metabolic analysis and engineering, and genetic engineering tools exist for realising favourable in silico strategies. As the glucose is the preferred substrate of both wild-type species, we utilised the engineered *E. coli* strain ZSC113 [60] that is unable to metabolise glucose because of gene deletions of the glucose and mannose ABC transporters and the enzyme hexokinase that catalyses the first reaction in glycolysis to ensure co-utilisation of the two substrates. This strain has been previously used in co-culture with a glucose-specific *E. coli* mutant to produce lactate from mixtures of glucose and xylose [61].

3.1.2 Model formulation: The co-culture stoichiometric matrix in (4) was constructed from the genome-scale metabolic reconstructions *S. cerevisiae* *i*ND750 [7] and *E. coli* *i*JR904 [59]. The wild-type *i*JR904 model was modified by constraining flux bounds for glucose exchange and glucose kinase at zero to mathematically represent the associated gene deletions. The steady-state flux balance model (5) was made dynamic through the addition of five extracellular mass balance equations describing the time evolution of the *S. cerevisiae* and ZSC113 biomass concentrations, the glucose concentration (G), the xylose concentration (Z) and the ethanol concentration (E). Oxygen mass balances were omitted under the reasonable assumption that the dissolved oxygen concentration (O)

doi: 10.1049/iet-syb.2013.0021

could be maintained at 0.1 mmol/l through aeration and agitation. Although *E. coli* can produce and consume acetate under aerobic conditions, we assumed that acetate was not produced at sufficient levels to affect the growth of the two microbes and that acetate consumption would not occur until xylose has been exhausted. Upper bounds on the sugar and oxygen uptake rates because of transport limitations were calculated using the following kinetic expressions

$$v_g = v_{g,\max}\frac{G}{K_g + G}\frac{1}{1+\frac{E}{K_{ieg}}} \tag{7}$$

$$v_z = v_{z,\max}\frac{Z}{K_z + Z}\frac{1}{1+\frac{E}{K_{iez}}} \tag{8}$$

$$v_o = v_{o,\max}\frac{O}{K_o + O} \tag{9}$$

where $v_{g,max}$, $v_{z,max}$ and $v_{o,max}$ are the maximum uptake rates of each substrate, K_g, K_z and K_o are the corresponding saturation constants, and K_{ieg} and K_{iez} are the ethanol inhibition constants. The oxygen uptake rate v_o was calculated with a constant dissolved oxygen concentration $O = 0.1$ mmol/l. Different oxygen uptake parameters were used for each organism. Under aerobic conditions *S. cerevisiae* can consume ethanol as a growth substrate after glucose is exhausted from the media, whereas *E. coli* is unable to metabolise ethanol [62]. As the ethanol diffuses freely across the plasma membrane [63], this behaviour was modelled by removing the lower bound on the ethanol exchange flux in the *S. cerevisiae* model. The amount of ethanol actually consumed in silico was determined by the amount of oxygen available. When grown in aerobic batch culture *S. cerevisiae* consumes glucose and produces ethanol oxido-fermentatively [64], whereas ethanol consumption by *S. cerevisiae* is purely respirative. Once the predicted glucose concentration dropped below 0.01 g/l, the value at which ethanol consumption was first observed

Table 1 Substrate uptake parameters for the dynamic flux balance model of *E. coli* ZSC113 and *S. cerevisiae* co-cultures

Parameter	*E. coli* ZSC113	*S. cerevisiae*
$v_{g,max}$, mmol/gdw/h	—	25.9
K_g, g/l	—	0.5
$v_{z,max}$, mmol/gdw/h	9	—
K_z, g/l	0.01	—
$K_{i,e}$, g/l	8	10
$v_{o,max}$, mmol/gdw/h	8	1.5[a]
K_o, mmol/l	0.001	0.003

[a]The $v_{o,max}$ was increased to 8.0 mmol/gdw/h for *S. cerevisiae* growth on ethanol.

experimentally, the maximum oxygen uptake rate was increased to reflect this change in metabolic phenotype.

3.1.3 Estimation of substrate uptake parameters:

Pure culture and co-culture dynamic flux balance models were solved by using the Mosek optimisation toolbox (Mosek ApS, Denmark) to resolve the LP for intracellular metabolism and the stiff differential equation solver ode15 s in Matlab (Mathworks, Natick, MA) to integrate the extracellular mass balance equations [24]. Sugar uptake parameters for each species were determined by trial-and-error as the combination of maximum uptake and saturation constants that minimised the least-squares error between the predicted and measured batch concentration profiles for anaerobic pure cultures. The *S. cerevisiae* ethanol inhibition constant (K_{ieg}) was fixed at the value used in our previous modelling study [13], whereas the glucose uptake parameters ($v_{g,max}$, K_g) were estimated from biomass, glucose and ethanol concentration profiles during the exponential growth phase. As the ZSC113 pure cultures did not produce sufficient ethanol to elicit an inhibitory response, only the parameters $v_{z,max}$ and K_z were adjusted to fit the biomass, xylose and ethanol concentration profiles. With the sugar uptake parameters held constant, the oxygen uptake parameters ($v_{o,max}$, K_o) for each species were found by trial-and-error minimisation of the least-squares error between predicted and measured batch concentration profiles for aerobic pure cultures. To model the

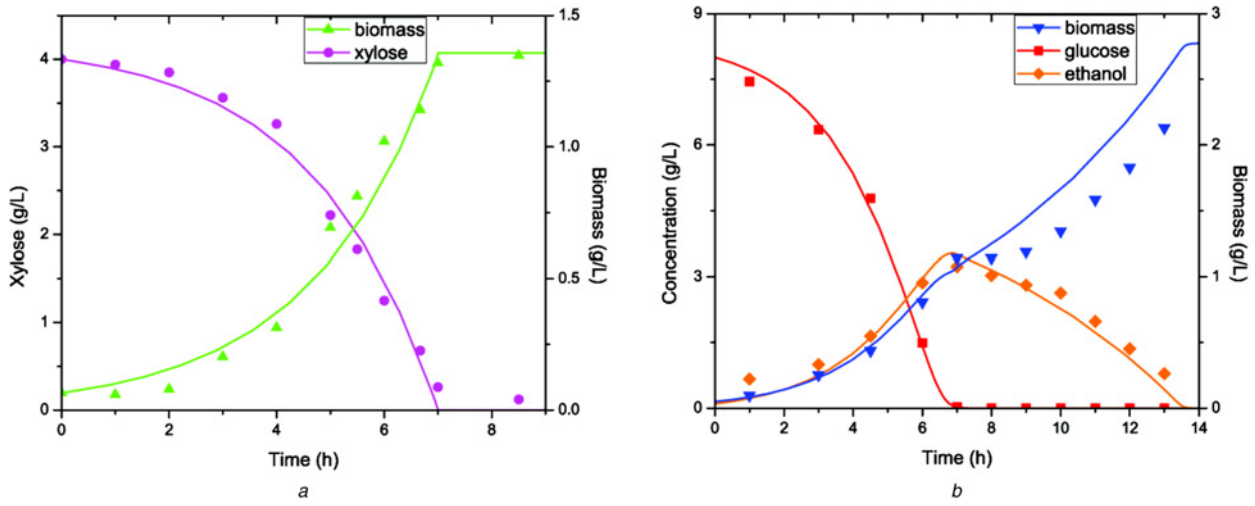

Fig. 4 *Experimental data (points) and best-fit pure culture model predictions with original NGAM values (solid lines) for aerobic batch fermentations performed at optimal growth conditions for each species.*

a E. coli ZSC113 grown at 37°C and pH 7
b S. cerevisiae grown at 30°C and pH 5

S. cerevisiae metabolic phenotype change that occurs following the switch to ethanol as the carbon source, the maximum oxygen uptake ($v_{o,max}$) was increased from 1.5 to 8.0 mmol/gdw/h for growth on ethanol [64]. The ethanol inhibition constant (K_{iez}) for ZSC113 xylose uptake was found by minimising the least-squares error between co-culture model predictions and ZSC113 biomass and xylose concentration profiles from a co-culture experiment where the ethanol concentration was sufficiently high to cause growth inhibition. The resulting parameter values are shown in Table 1.

3.1.4 Pure cultures at optimal growth conditions:

Following the procedure shown in Fig. 3, we first conducted pure culture batch experiments at the optimal growth conditions of each species to estimate substrate uptake parameters and to access the pure culture dynamic flux balance models. These fermentations were performed at 30°C and pH 5 for *S. cerevisiae* and at 37°C and pH 7 for ZSC113. A comparison of measured concentration profiles and corresponding model predictions for aerobic batch cultures of *S. cerevisiae* and ZSC113 are shown in Fig. 4. The ZSC113 model predictions (Fig. 4*a*) were very satisfactory with only small differences observed between the measured and predicted profiles. An ethanol concentration profile was not shown for this case because *E. coli* does not produce this metabolic by-product under aerobic conditions. The *S. cerevisiae* model predictions (Fig. 4*b*) were very good with the exception of the biomass concentration following the transition from glucose to ethanol as the carbon source because the diauxic lag was not captured by the model. However, the goal of this study was to engineer the co-culture system such that glucose and xylose were simultaneously exhausted and ethanol was not consumed.

3.1.5 Identification of co-culture growth conditions:

As the *S. cerevisiae* and *E. coli* do not share the same optimal growth conditions, a common temperature and pH for co-culturing the two species was determined. Rather than explicitly model the growth rate of each species through the development of empirical models of the form $\mu = f(\text{pH},T)$ as is common in unstructured modelling [16], the co-culture conditions were experimentally determined as the temperature and pH that maximised the normalised biomass productivity. The biomass productivity of each species was determined by dividing the individual species biomass produced in co-culture by the time required to

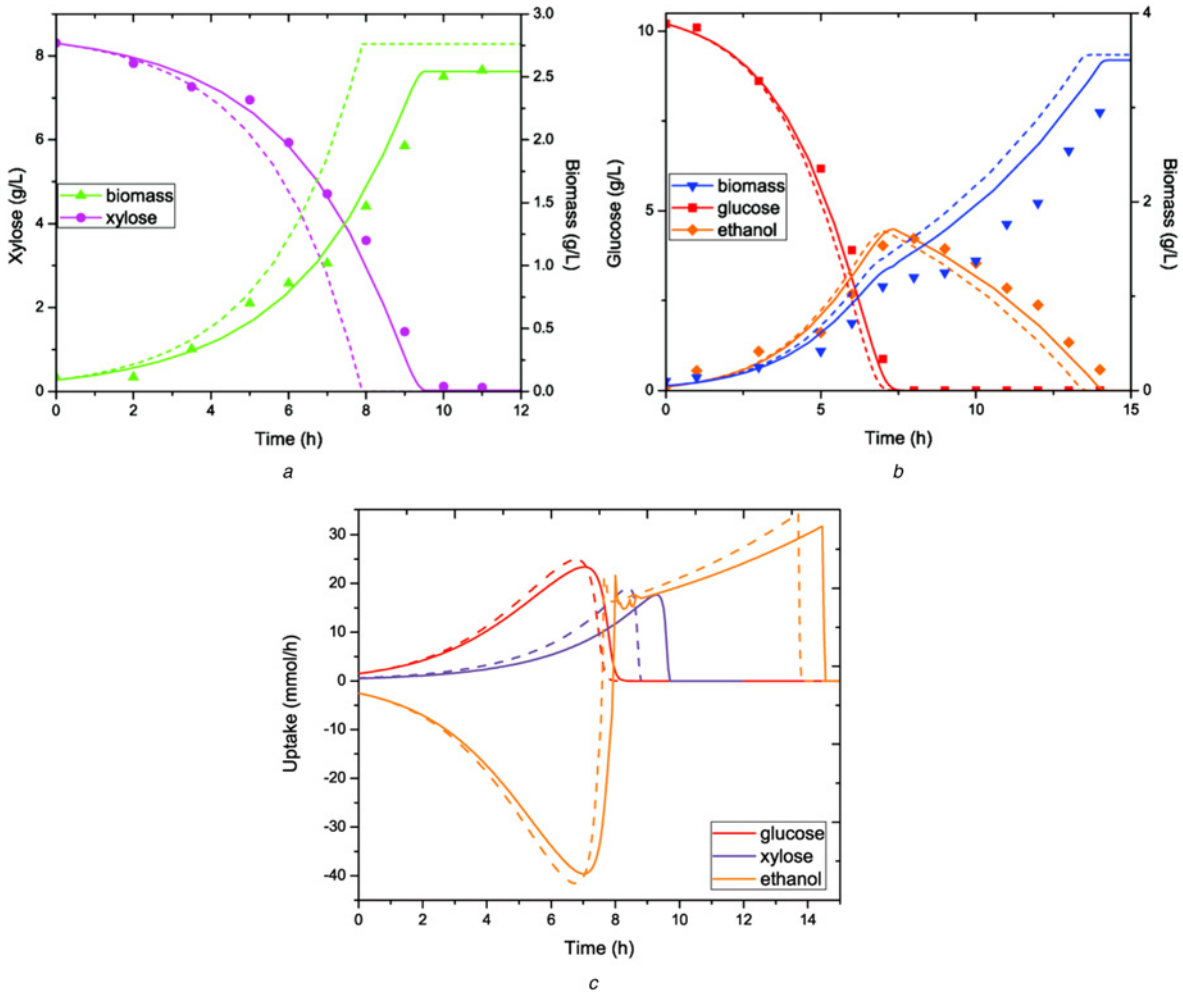

Fig. 5 *Experimental data (points), pure culture model predictions with original NGAM values (dashed lines) and best-fit pure culture model predictions with optimised NGAM values (solid lines) for aerobic batch fermentations performed at suboptimal growth conditions (32.5°C and 5.5 pH) for each species.*

a E. coil ZSC113 predictions obtained by increasing NGAM from 7.6 to 10.5 mmol/gdw/h
b S. cerevisiae predictions obtained by increasing NGAM from 1.0 to 3.6 mmol/gdw/h
c Rates of glucose and xylose uptake and ethanol secretion/uptake for the simulations in (a) and (b)

doi: 10.1049/iet-syb.2013.0021

reach the stationary phase. The normalised biomass productivity of each species was calculated by dividing the biomass productivity for a particular co-culture growth condition by the biomass productivity obtained for the optimal growth condition in pure culture. The total normalised biomass productivity was defined as the sum of the two individual values. Co-culture fermentations inoculated with 0.05 g/l of each species and initiated with 16 g/l glucose and 8 g/l xylose were conducted over a range of temperatures between 30 and 37°C and pH values between 5 and 7, respectively. We found that the best common growth conditions corresponded to a temperature of 32.5°C and a pH of 5.5. This combination produced a normalised biomass productivity of 1.7, only 15% below the maximum possible value of 2. We found that both *S. cerevisiae* and *E. coli* ZSC113 were most sensitive to pH, perhaps because of the strong effect of pH on the energy each species had to expend to establish and maintain the proton motive force. The identified pH was closest to the *S. cerevisiae* optimum, most likely because the yeast TCA cycle operates most efficiently in the pH range 4–6 [65].

3.1.6 Pure cultures at co-culture growth conditions: We investigated two methods for adapting the pure culture models to the identified co-culture growth conditions. The first approach involved re-estimating the substrate uptake parameters from batch fermentation data collected at the suboptimal conditions. Although this approach generated models that could accurately reproduce the concentration profiles used for estimation, unsatisfactory predictions were obtained when the models were validated with other glucose/xylose concentrations (not shown). We found that more accurate predictions over a range of initial substrate concentrations could be obtained by increasing the non-growth associated maintenance (NGAM) within the flux balance models for each species while leaving the substrate uptake parameters fixed at the values estimated at optimal growth conditions. Although this approach was not mechanistic, the microbes were expected to be less energetically efficient at suboptimal growth conditions [15]. Fig. 5 shows a comparison of predicted concentration profiles obtained with the original NGAM values and those obtained with optimised NGAM values for pure batch cultures conducted at the common, suboptimal conditions

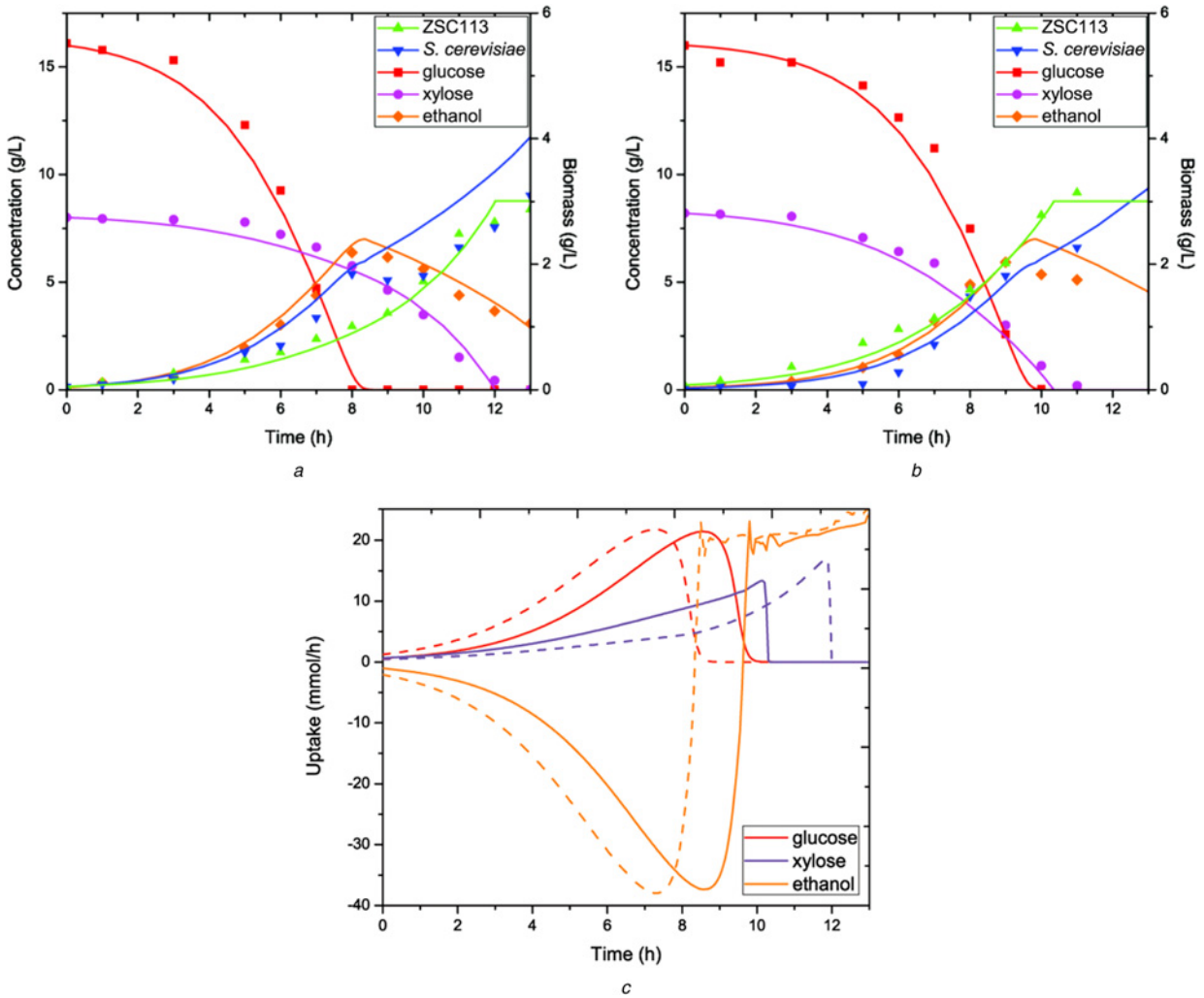

Fig. 6 *Experimental data (points) and co-culture model predictions (solid lines) for aerobic batch fermentations with 0.1 g/l total inoculum for a sugar mixture of 16 g/l glucose and 8 g/l xylose.*

a Equal inoculum with 0.05 g/l of each microbe
b Optimised inoculum with 0.027 g/l *S. cerevisiae* and 0.073 g/l *E. coli* ZSC113
c Rates of glucose and xylose uptake and ethanol secretion/uptake for equal inoculum (dashed lines) and optimised inoculum (solid lines)

of 32.5°C and 5.5 pH. For each species, the optimised results were obtained by manually adjusting the NGAM value such that the least-squares error between the predicted and measured profiles was minimised. The necessary adjustments from the original values were 7.6–10.5 mmol/gdw/h for *E. coli* ZSC113 and 1.0–3.6 mmol/gdw/h for *S. cerevisiae*. Owing to increased non-growth associated consumption of energy, we observed reduced substrate uptake rates, slower growth rates and longer batch times at the suboptimal conditions. The model fits shown in Fig. 5 are comparable with those in Fig. 4 for pure cultures at optimal growth conditions. Furthermore, the pure culture models with adjusted NGAM values were extensible to other substrate mixtures (shown below).

3.1.7 Co-cultures with equal inoculum: Owing to the large difference in cell size between *E. coli* and *S. cerevisiae*, the individual concentrations of the two species were determined by particle size distribution measurement. The two species were co-cultured at the identified co-culture conditions with an equal inoculum of 0.05 g/l of each organism. The co-culture dynamic flux balance model generated directly from the two pure culture models generated satisfactory predictions of *S. cerevisiae* metabolism modulo the diauxic lag (Fig. 6*a*), suggesting that *S. cerevisiae* was largely uninfluenced by the presence of ZSC113. Recognising that ZSC113 was exposed to moderate concentrations of ethanol in co-culture and that ethanol is a known inhibitor of *E. coli* growth, we incorporated an ethanol inhibition term into the ZSC113 xylose uptake rate. The ZSC113 predictions in Fig. 6*a* generated with the ethanol inhibition constant $K_{ie} = 8.0$ g/l produced excellent agreement with experiment, suggesting that this simple modification was sufficient to capture the observed species interactions.

3.1.8 Inoculum optimisation: As the batch co-culture experiment shown in Fig. 6*a* was performed with an equal inoculum, glucose was consumed much faster by *S. cerevisiae* than xylose was consumed by ZSC113. Since the co-culture model was able to generate accurate predictions up to the diauxic switch, we used the model for in silico determination of an optimal inoculum that would produce simultaneous exhaustion of the two sugars. For this purpose, the batch time was defined as the time at which xylose was predicted to be 85% consumed. For a total inoculum concentration of 0.1 g/l, the co-culture model predicted that an inoculum of 0.027 g/l *S. cerevisiae* and 0.073 g/l ZSC113 would yield simultaneous exhaustion of 16 g/l glucose and 8 g/l xylose at 9.8 h. This prediction proved to be highly accurate, as the validation experiment performed also resulted in a batch time of 9.8 h (Fig. 6*b*). The co-culture model produced satisfactory predictions of all concentration profiles up to the *S. cerevisiae* diauxic shift to growth on ethanol following sugar exhaustion. Fig. 6*C* shows that the optimised inoculum produced faster xylose uptake rates at the expense of slower glucose uptake. As an unoptimised inoculum with equal species concentrations produced a batch time of 11.5 h, the optimisation procedure generated a 15% decrease in batch time and a corresponding increase in the productivity of substrate consumption. Similar results were obtained for sugar mixtures of 12 g/l glucose, 12 g/l xylose and 8 g/l glucose, 16 g/l xylose (Table 2). These results demonstrate extensibility of the co-culture model to different initial cell and substrate concentrations.

3.2 Biomass hydrolysate detoxification by *S. cerevisiae*/*S. stipitis* co-cultures

3.2.1 Strain selection: In this study [41], we focused on the problem of growth inhibitor detoxification with a co-culture system comprised a respiratory-deficient *S. cerevisiae* mutant and the xylose-consuming yeast *S. stipitis*. *S. cerevisiae* 311, a mutant that was created by treating a wild-type strain with ethidium bromide [66], was selected as the respiratory-deficient *S. cerevisiae* strain. The wild-type *S. stipitis* strain NRRL Y-7124 was used in this study. In addition to sharing the same optimal growth conditions of 30°C and pH of 5 [67], these two species can be co-cultured to produce larger amounts of ethanol from glucose and xylose mixtures than either yeast in pure culture [68, 69]. The use of respiratory deficient *S. cerevisiae* prevents the aerobic re-assimilation of ethanol and allows for more precise regulation of oxygen levels needed to establish microaerobic conditions under which *S. stipitis* has high ethanol synthesis capabilities [70]. Chemical pretreatment of biomass for conversion to renewable chemicals typically produces furan compounds that can significantly inhibit the metabolism of microorganisms such as *S. cerevisiae* and *S. stipitis* [71]. Both *S. cerevisiae* and *S. stipitis* have the capacity to reduce toxic furan compounds to their corresponding alcohols [72] and detoxify their culture environment. Of particular interest in this study was the reduction of furfural to furfuryl alcohol and the conversion of 5-hydroxymethyl furfural (HMF) to 2,5-bis-hydroxymethylfuran because these furans are commonly present in biomass hydrolysates [73, 74].

3.2.2 Model development: Flux balance models based on the *i*MM904 *S. cerevisiae* [75] and *i*BB814 *S. stipitis* [6] metabolic reconstructions were used to model the effects of furan inhibitors. To model the respiratory deficiency of *S. cerevisiae* 311, the ubiquinol-6 cytochrome c reductase and mitochondrial cytochrome c oxidase catalysed reactions were deleted from the *i*MM904 network. Deletion of

Table 2 Comparison of experimental and predicted co-culture batch times for equal and optimised inoculums of *E. coli* ZSC113 and *S. cerevisiae*

Sugar mixture (g glucose/g xylose)	Unoptimised			Optimised			Batch time reduction, %	
	Inoculum (g *S. cerevisiae*/g ZSC113)	Batch time, h		Inoculum (g *S. cerevisiae*/g ZSC113)	Batch time, h			
		Experiment	Model		Experiment	Model	Experiment	Model
16/8	0.05/0.05	11.6	11.5	0.027/0.073	9.8	9.8	15.5	14.9
12/12	0.05/0.05	11.8	12.5	0.0125/0.0875	9.9	10.3	16.1	18.2
8/16	0.05/0.05	12.7	12.8	0.0075/0.0925	10.9	10.4	14.2	18.6

doi: 10.1049/iet-syb.2013.0021

these two reactions prevented the use of pathways in the mitochondria responsible for respiratory metabolism and rendered the *S. cerevisiae* model unable to grow on ethanol. Furfural and HMF metabolism where incorporated in the published *S. cerevisiae* and *S. stipitis* networks by: (i) adding uptake and secretion reactions for the metabolites furfural, HMF, furfuryl alcohol and 2,5-bis-hydroxymethylfuran; and (ii) adding the following intracellular reduction reactions

$$1\ \text{furfural} + 1/2\ \text{NADPH} + 1/2\ \text{NADH} - - > 1\ \text{furfuryl alcohol} + 1/2\ \text{NADP} + 1/2\ \text{NAD}^{+} \quad (10)$$

$$1\ \text{HMF} + 1/2\ \text{NADPH} + 1/2\ \text{NADH} - - > 12,5\text{-bis-hydroxymethylfuran} + 1/2\ \text{NADP} + 1/2\ \text{NAD}^{+} \quad (11)$$

As the inhibitors are known to be reduced by a combination of enzymes with different cofactor preferences, both yeasts were assumed to use equal amounts of NADH and NADPH in the detoxification process [76]. Although *S. cerevisiae* has been shown to produce acetate during HMF reduction [77], the *S. cerevisiae* model did not produce experimentally observed amounts of acetate unless modified. The model was forced to produce more acetate by constraining the network to recover all reducing equivalents lost to HMF reduction through the aldehyde dehydrogenase reaction that produces acetate from acetaldehyde.

Extracellular mass balances on *S. cerevisiae* biomass, *S. stipitis* biomass, glucose, xylose, ethanol and liquid- and gas-phase oxygen were added to the steady-state flux balance models to simulate batch co-culture growth. Five additional extracellular mass balances on furfural (F), 2,5-bis-hydroxymethylfuran (HMF), furfuryl alcohol, 2,5-bis-hydroxymethylfuran and acetate (A) were added to account for the uptake and secretion of inhibitory compounds. Acetate was assumed to be produced only by *S. cerevisiae* in the presence of HMF, but both species were able to uptake acetate for growth. In addition to sugar uptake kinetics of the general form shown in (7)–(9), the

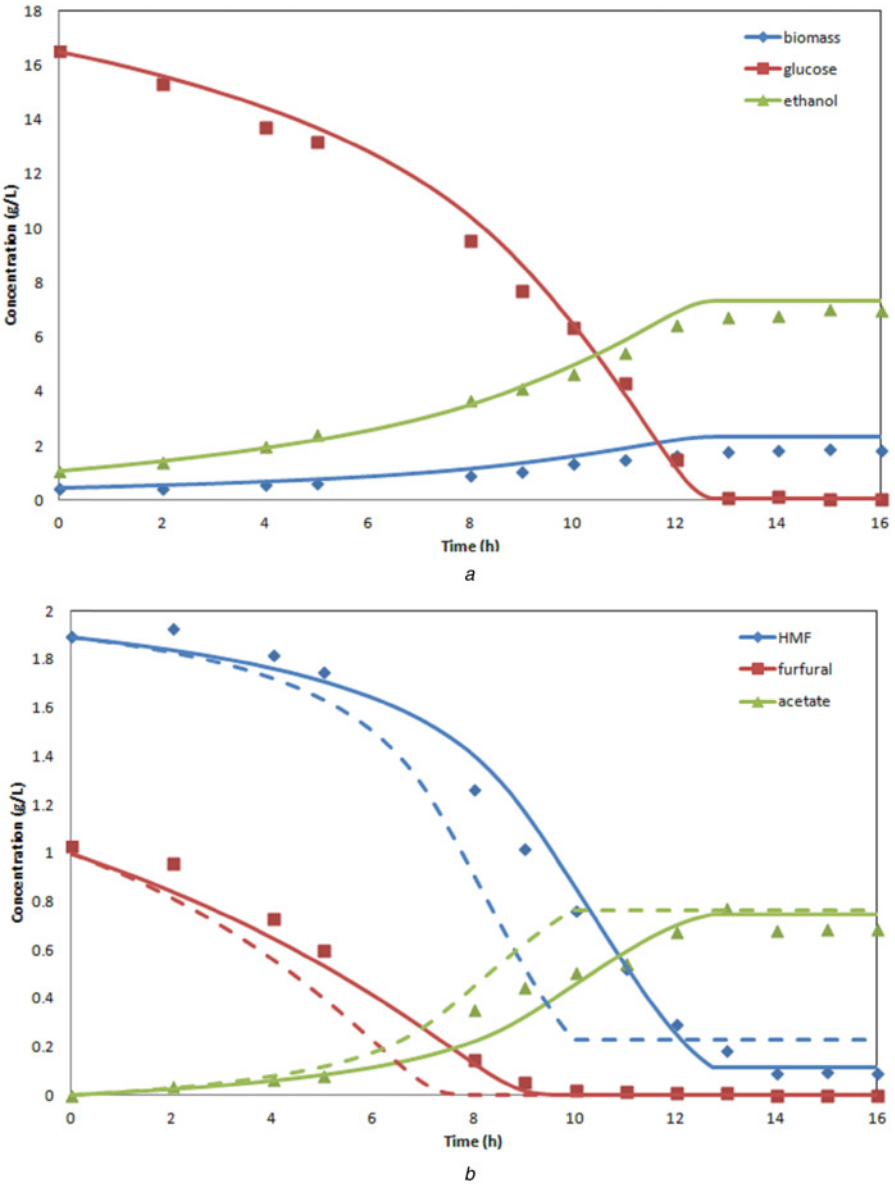

Fig. 7 *S. cerevisiae 311 batch fermentation for growth on 16.5 g/l glucose with 1 g/l furfural and 1.89 g/l HMF. Points represent experimental data, and solid and dashed lines are model predictions with and without a term for furfural inhibition on HMF uptake, respectively.*

following inhibitor uptake kinetics were incorporated into the dynamic flux balance models

$$v_{\mathrm{f}} = v_{\mathrm{f,max}} \frac{F}{K_{\mathrm{f}} + F} \tag{12}$$

$$v_{\mathrm{hmf}} = v_{\mathrm{hmf,max}} \frac{\mathrm{HMF}}{K_{\mathrm{hmf}} + \mathrm{HMF}} \frac{1}{1 + \dfrac{F}{K_{\mathrm{if,hmf}}}} \tag{13}$$

$$v_a = v_{a,\max} \frac{A}{K_a + A} \tag{14}$$

The Michaelis–Menten kinetics for HMF uptake were modified by a term reflecting the cellular preference for furfural detoxification. All other inhibition terms added to modify sugar and inhibitor uptake kinetics had the form

$$\frac{1}{1 + \dfrac{J}{K_{ij,k}}} \tag{15}$$

where J is the concentration of the inhibiting compound j and $K_{ij,k}$ is the inhibition constant for compound j inhibiting the uptake of species k. The resulting pure and co-culture dynamic flux balance models were solved using the MOSEK LP solver coupled to the Matlab ODE solver ode15 s.

3.2.3 S. cerevisiae pure cultures: Batch fermentations of *S. cerevisiae* 311 with glucose as the carbon source in the presence of either furfural or HMF were conducted to quantify the effects of these inhibitory compounds on *S. cerevisiae* metabolism. As including only the drain on reducing equivalents shown in (10) and (11) proved insufficient to model batch fermentations with either inhibitor, a term of the form in (15) that captured the inhibition of each furan aldehyde on glucose uptake was added to the model. Although this modification adequately described *S. cerevisiae* growth in the presence of HMF, the rate of glucose consumption remained overpredicted. Therefore inhibitory terms for furfuryl alcohol and acetate were added to the glucose uptake kinetics. The resulting pure culture model was validated by comparing model predictions and batch fermentation data for *S. cerevisiae* growing on glucose in the presence of both furfural and HMF (Fig. 7). As the model predicted faster reduction of HMF than was observed in experiment, a term for inhibition of HMF uptake by furfural was added as shown in (13). A slight overprediction of ethanol and biomass yields observed in single inhibitor fermentations (not shown) is also seen in Fig. 7. The estimated model parameters related to sugar and inhibitor uptake by *S. cerevisiae* 311 are shown elsewhere [41].

3.2.4 S. stipitis pure cultures: Batch fermentations of *S. stipitis* with either glucose or xylose as the carbon source in the presence of both furfural and HMF were conducted to quantify the effects of these inhibitory compounds on *S. stipitis* metabolism. Satisfactory fits of experimental data were obtained by incorporating inhibition terms for furfural and furfuryl alcohol into the uptake kinetics of both glucose and xylose. The addition of terms for HMF inhibition of the glucose and xylose uptake kinetics further improved agreement with our data. However, our best parameter fits did not fully capture the split between cell growth and ethanol production in *S. stipitis* as the ethanol concentration was under-predicted in glucose media and the biomass concentration was under-predicted in xylose media. The parameter values obtained for glucose and xylose media were evaluated by co-fermentation of both sugars in the presence of both inhibitors (Fig. 8). Although the dynamic model generally produced satisfactory transient predictions, the same discrepancies between model and experiment observed in single sugar fermentations were seen in co-fermentation of the two sugars. Despite these deficiencies, the model was able to generate very accurate predictions of the final biomass and ethanol yields. In preparation for modelling co-cultures of *S. cerevisiae* 311 and *S. stipitis*, the effect of acetate on *S. stipitis* metabolism was investigated. The *S. stipitis* dynamic model was modified by adding acetate uptake and a term for acetate inhibition of the xylose uptake rate. This modified model produced good qualitative agreement with fermentation data for acetate-containing xylose media until approximately 40

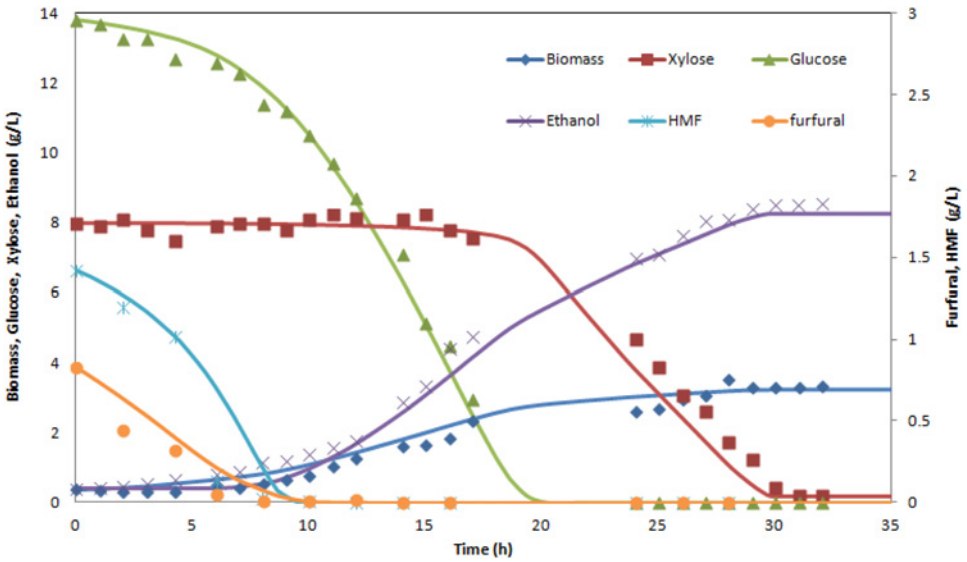

Fig. 8 *S. stipitis batch fermentation for growth on 13.8 g/l glucose and 8.0 g/l xylose with 0.83 g/l furfural and 1.42 g/l HMF. Points represent experimental data and solid lines are model predictions.*

doi: 10.1049/iet-syb.2013.0021

h into the batch, at which time *S. stipitis* growth stopped despite the availability of xylose (not shown). This unmodelled effect was possibly because of a combination of cumulative cellular damage induced by reactive oxygen species and the inhibitory effect of ethanol [78]. The estimated model parameters related to sugar and inhibitor uptake by *S. stipitis* are shown elsewhere [41].

3.2.5 S. cerevisiae/S. stipitis co-cultures: As the *S. cerevisiae* and *S. stipitis* have similar cell sizes that could not be differentiated by particle size analysis, cell counts were performed on a hemacytometer in triplicate and averaged to determine the individual species concentrations. Predictions from the co-culture dynamic flux balance model were compared with the experimental data collected from batch cultures inoculated with equal amounts of *S. cerevisiae* 311 and *S. stipitis* (Fig. 9). A version of the co-culture model that neglects inhibitors [42] yielded very poor predictions, whereas the developed co-culture model with inhibitor effects generally provided good agreement with our data. As observed in *S. stipitis* pure culture with acetate, cell growth stopped before xylose was completely consumed. These results suggest that either acetate alone or the cumulative effect of all the inhibitors induced changes to *S. stipitis* metabolism [79] that are not captured by the model. As the genome-scale metabolic reconstructions are charge balanced at the optimal pH for species growth, the intercellular acidification induced by acetate would be expected to make model predictions less accurate [80]. We found that doubling the *S. stipitis* ATP NGAM value was sufficient to stop cell growth in silico at the xylose, ethanol and acetate concentrations where the fermentation stalled in

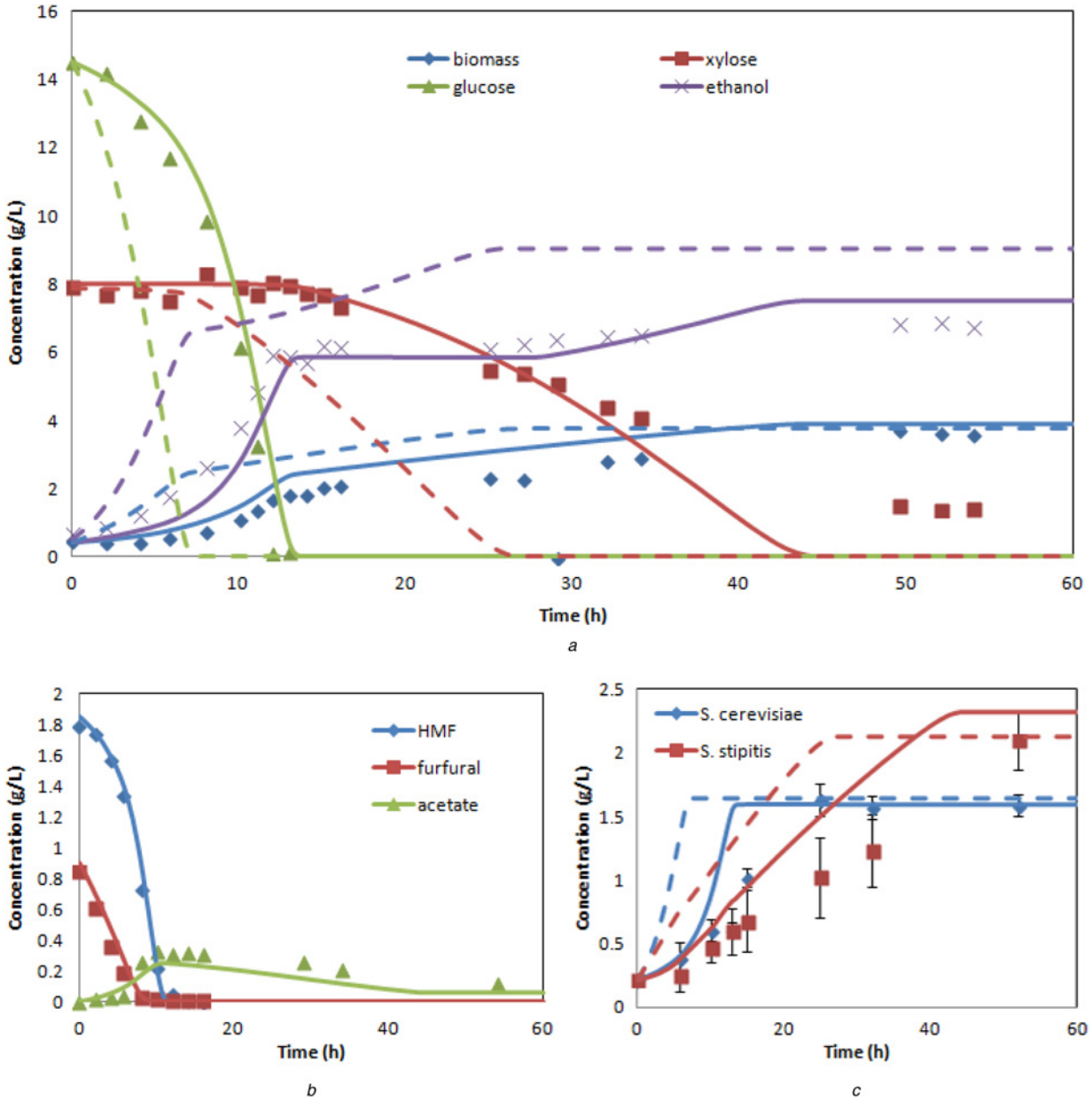

Fig. 9 *Co-culture dynamic flux balance model predictions for an equal inoculum. Points represent experimental data, dashed lines are model predictions without inhibitor modelling, and solid lines are model predictions with inhibitor modelling.*

a Metabolite and biomass concentrations
b Inhibitor concentrations
c Individual cell counts for an equal inoculum co-culture consuming 14.5 g/l glucose and 8 g/l xylose in the presence of 0.9 g/l furfural and 1.85 g/l HMF

Fig. 9. This severe inhibition of xylose metabolism by acetate emphasises the importance of removing acetate from lignocellulosic hydrolysates. Fig. 10 shows that the co-culture model produced greatly improved predictions for a 10/90 *S. cerevisiae*/*S. stipitis* inoculum ratio, most likely because of the much smaller amount of acetate produced by *S. cerevisiae*. A possible strategy for improving mixed-culture performance would be to introduce a third yeast species that is capable of removing acetate from the culture media without introducing other antagonistic effects on *S. cerevisiae* and *S. stipitis* [81].

4 Conclusions and future directions

DFBA is an emerging framework to simulate, analyse and optimise synthetic microbial communities for various biotechnological tasks. Compared with alternative modelling approaches, DFBA offers the important advantage that genome-scale metabolic reconstructions of individual species can be directly incorporated in the dynamic model. On the other hand, the approach is limited to communities in which the necessary metabolic reconstructions are available or can be developed. As a result, practical application of DFBA is currently restricted to synthetic communities comprised a few well-characterised species. The two case studies presented here focused on the development and validation of predictive dynamic models of co-culture systems for which curated metabolic models were available for the individual species. An important topic for future study is the rapid development of metabolic reconstructions for unmodelled microbial species, either identified as possible synthetic

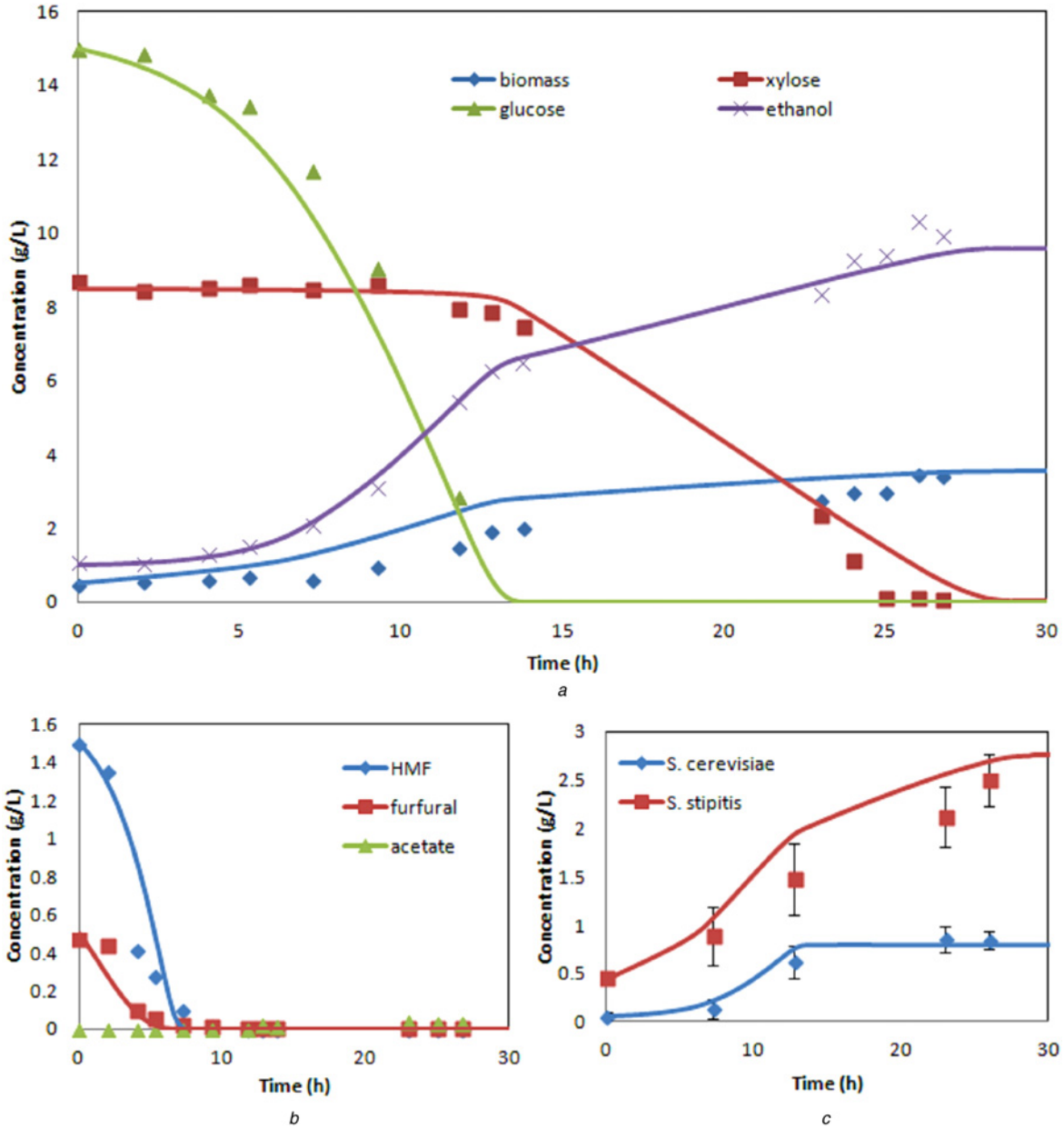

Fig. 10 *Co-culture dynamic flux balance model predictions for a 10% / 90% S. cerevisiae / S. stipitis inoculum, consuming 15 g/l glucose and 8.7 g/l xylose in the presence of 0.5 g/l furfural and 1.5 g/l HMF.*

a Metabolite and biomass concentrations
b Inhibitor concentrations
c Individual cell counts for a co-culture initiated with an inoculum of 10% *S. cerevisiae* 311 and 90% *S. stipitis*

doi: 10.1049/iet-syb.2013.0021

community members or isolated from natural microbial communities. The recent development of automated pipelines for metabolic reconstruction from annotated genomes [46–48] is a positive step in this direction.

A steady-state community flux balance model is formulated by combining the stoichiometric matrices of the individual species into a combined matrix and assuming an objective for the community such that the unknown fluxes can be calculated by solving a LP. As shown in the two case studies this procedure is straightforward if the community is assumed to maximise its total growth rate, which represents a multispecies extension of classical FBA for single species. Recently developed computational algorithms such as OptCom [51] allow the incorporation of species-level fitness criteria as well as community-level growth optimisation. Future research should include the development of combined experimental/computational methods for identifying species- and community-level objectives.

A community dynamic flux balance model is developed by combining the steady-state flux balance model described above with: (i) uptake kinetics for supplied substrates as well as exchanged metabolites; and (ii) extracellular mass balances on these substrates and metabolites as well as other important secreted products. The formulation of extracellular balance equations is straightforward and generally does not require fermentation data for parameter estimation. By contrast, substrate uptake kinetics are problem dependent and invariably require pure culture data for identification of the proper functional forms and estimation of unknown parameters. This identification problem is tractable for simple communities with a relatively small number of species, substrates and exchanged metabolites. For example, the second case study focusing on biomass hydrolysate detoxification involved two species (*S. cerevisiae* and *S. stipitis*), five substrates (glucose, xylose, oxygen, furfural and HMF) and one exchanged metabolite (acetate). However, the identification procedure can become very time consuming for more complex communities with larger numbers of species-substrate/metabolite pairs. The development of more efficient uptake identification methods, possibly enabled by highly parallel fermentation systems [82], would be a fruitful area for future research.

Robust and efficient numerical solution methods are needed for parameter estimation as well as dynamic simulation and optimisation of dynamic flux balance models. Although we have found that repeated solution of the LP representing intracellular metabolism within the solution of the extracellular differential equations is satisfactory for co-culture models, specialised solution methods may be needed for more complex community models and/or computational tasks. A solution algorithm recently developed for single-species DFBA that is based on reformulating the model as differential-algebraic equation system [54] is promising and warrants extension to multispecies models. Incorporation of the necessary tools for species genome annotation and metabolic reconstruction, substrate uptake identification, community dynamic modelling, and dynamic simulation and optimisation within a single software platform would be very beneficial. The recent release of the Model SEED within the DOE Systems Biology Knowledgebase (KBase) is a positive step in this direction, and plans to expand KBase to microbial communities are under development.

Applications of DFBA have been limited to small synthetic microbial communities for which the necessary genome-scale metabolic models are available or can be developed. Such communities have application to important biotechnological tasks such as degradation of lignocellulosic feedstocks and conversion of complex sugar mixtures. However, natural microbial communities are considerably more complex because they are comprised numerous species that exhibit a broad range of unknown interactions. A future research goal should be extension of the DFBA approach to natural communities comprised of novel species that lack genome-scale metabolic reconstructions. One possible approach is to isolate and sequence the dominant species of the community [83], such that genome-scale reconstructions could be developed for these species using an automated model generation tool. Then a suitable extension of the co-culture modelling framework shown in Fig. 3 could be developed for community modelling. Alternatively, the entire community could be sequenced and the resulting metagenome could be used to identify and develop genome-scale reconstructions of representative species classes. This approach would require culturing of representative model species to develop the necessary update kinetics and species interactions for dynamic flux balance model construction. Although platforms such as KBase currently under development may eventually provide such capabilities, considerable research is needed to realise the individual components of such an integrated community model development platform.

5 Acknowledgment

This work was partially supported by the NSF-sponsored UMass Institute for Cellular Engineering IGERT programme (Grant number DGE-0654128) and ReCommunity Recycling. The authors wish to thank Dr. Swati Khanna for her assistance in compiling the references.

6 References

1 Kauffman, K.J., Prakash, P., Edwards, J.S.: 'Advances in flux balance analysis', *Curr. Opin. Biotechnol.*, 2003, **14**, (5), pp. 491–496.
2 Palsson, B.Ø.: 'Systems biology: properties of reconstructed networks' (Cambridge University Press, 2006)
3 Schuetz, R., Kuepfer, L., Sauer, U.: 'Systematic evaluation of objective functions for predicting intracellular fluxes in Escherichia coli', *Mol. Syst. Biol.*, 2007, **3**, p. 119
4 Santos, F., Boele, J., Teusink, B.: 'A practical guide to genome-scale metabolic models and their analysis', *Methods Enzymol.*, 2011, **500**, pp. 509–32
5 Thiele, I., Palsson, B.Ø.: 'A protocol for generating a high-quality genome-scale metabolic reconstruction', *Nat. Protoc.*, 2010, **5**, (1), pp. 93–121
6 Balagurunathan, B., Jonnalagadda, S., Tan, L., Srinivasan, R.: 'Reconstruction and analysis of a genome-scale metabolic model for *Scheffersomyces stipitis*', *Microbial Cell Factories*, 2012, **11**, (1), p. 27
7 Duarte, N.C., Herrgård, M.J., Palsson, B.Ø.: 'Reconstruction and validation of *Saccharomyces cerevisiae* iND750, a fully compartmentalized genome-scale metabolic model', *Genome Res.*, 2004, **14**, (7), pp. 1298–1309
8 Bro, C., Regenberg, B., Forster, J., Nielsen, J.: 'In silico aided metabolic engineering of *Saccharomyces cerevisiae* for improved bioethanol production', *Metab. Eng.*, 2006, **8**, pp. 102–111
9 Pharkya, P., Maranas, C.D.: 'An optimization framework for identifying reaction activation/inhibition or elimination candidates for overproduction in microbial systems', *Metab. Eng.*, 2006, **8**, (1), pp. 1–13
10 Roberts, S., Gowen, C., Brooks, J.P., Fong, S.: 'Genome-scale metabolic analysis of *Clostridium thermocellum* for bioethanol production', *BMC Syst. Biol.*, 2010, **4**, (1), p. 31

11 Segrè, D., Vitkup, D., Church, G.M.: 'Analysis of optimality in natural and perturbed metabolic networks', *Proc. Natl. Acad. Sci.*, 2002, **99**, (23), pp. 15112–15117
12 Becker, S.A., Feist, A.M., Mo, M.L., Hannum, G., Palsson, B.Ø., Herrgard, M.J.: 'Quantitative prediction of cellular metabolism with constraint-based models: the COBRA Toolbox', *Nat. Protoc.*, 2007, **2**, (3), pp. 727–738
13 Hjersted, J.L., Henson, M.A.: 'Optimization of fed-batch *Saccharomyces cerevisiae* fermentation using dynamic flux balance models', *Biotechnol. Prog.*, 2006, **22**, (5), pp. 1239–1248
14 Mahadevan, R., Edwards, J.S., DoyleIIIF.J.: 'flux balance analysis of diauxic growth in *Escherichia coli*', *Biophys. J.*, 2002, **83**, (3), pp. 1331–1340
15 Meadows, A.L., Karnik, R., Lam, H., Forestell, S., Snedecor, B.: 'Application of dynamic flux balance analysis to an industrial *Escherichia coli* fermentation', *Metab. Eng.*, 2010, **12**, (2), pp. 150–160
16 Bailey, J.E., Ollis, D.E.: 'Biochemical engineering fundamentals' (McGraw-Hill, New York, NY, 1986, 2nd edn.)
17 Steinmeyer, D.E., Shuler, M.L.: 'Structured model for *Saccharomyces cerevisiae*', *Chem. Eng. Sci.*, 1989, **44**, (9), pp. 2017–2030
18 Vaseghi, S., Baumeister, A., Rizzi, M., Reuss, M.: 'In vivo dynamics of the pentose phosphate pathway in *Saccharomyces cerevisiae*', *Metab. Eng.*, 1999, **1**, (2), pp. 128–40
19 Hatzimanikatis, V., Emmerling, M., Sauer, U., Bailey, J.E.: 'Application of mathematical tools for metabolic design of microbial ethanol production', *Biotechnol. Bioeng.*, 1998, **58**, (2–3), pp. 154–161
20 Jones, K.D., Kompala, D.S.: 'Cybernetic model of the growth dynamics of *Saccharomyces cerevisiae* in batch and continuous cultures', *J. Biotechnol.*, 1999, **71**, (1–3), pp. 105–131
21 Varner, J., Ramkrishna, D.: 'Nonlinear analysis of cybernetic models. Guidelines for model formulation', *J. Biotechnol.*, 1999, **71**, pp. 67–103
22 Akesson, M., Forster, J., Nielsen, J.: 'Integration of gene expression data into genome-scale metabolic models', *Metab. Eng.*, 2004, **6**, pp. 285–293
23 Blazier, A.S., Papin, J.A.: 'Integration of expression data in genome-scale metabolic network reconstructions', *Front Physiol.*, 2012, **3**, p. 299
24 Hjersted, J.L., Henson, M.A.: 'Steady-state and dynamic flux balance analysis of ethanol production by *Saccharomyces cerevisiae*', *IET Syst. Biol.*, 2009, **3**, (3), pp. 167–179
25 Brenner, K., You, L., Arnold, F.H.: 'Engineering microbial consortia: a new frontier in synthetic biology', *Trends Biotechnol.*, 2008, **26**, (9), pp. 483–489
26 Alper, H., Stephanopoulos, G.: 'Engineering for biofuels: exploiting innate microbial capacity or importing biosynthetic potential?', *Nat. Rev. Micro.*, 2009, **7**, (10), pp. 715–723
27 Handelsman, J.: 'Sorting out metagenomes', *Nat. Biotechnol.*, 2005, **23**, (1), pp. 38–39
28 Meyer, F., Paarmann, D., D'Souza, M., Olson, R., Glass, E.M., *et al.*: 'The metagenomics RAST server – a public resource for the automatic phylogenetic and functional analysis of metagenomes', *BMC Bioinformatics*, 2008, **9**, p. 386
29 Hess, M., Sczyrba, A., Egan, R., Kim, T.-W., Chokhawala, H., *et al.*: 'Metagenomic discovery of biomass-degrading genes and genomes from cow rumen', *Science*, 2011, **331**, (6016), pp. 463–467
30 Suen, G., Teiling, C., Li, L., Holt, C., Abouheif, E., *et al.*: 'The genome sequence of the leaf-cutter ant Atta cephalotes reveals insights into its obligate symbiotic lifestyle', *PLoS Genet.*, 2011, **7**, (2), p. e1002007
31 Woyke, T., Teeling, H., Ivanova, N.N., Huntemann, M., *et al.*: 'Symbiosis insights through metagenomic analysis of a microbial consortium', *Nature*, 2006, **443**, (7114), pp. 950–955
32 Klitgord, N., Segre, D.: 'Ecosystems biology of microbial metabolism', *Curr. Opin. Biotechnol.*, 2011, **22**, pp. 1–6
33 Khandelwal, R.A., Olivier, B.G., Röling, W.F.M., Teusink, B., Bruggeman, F.J.: 'Community flux balance analysis for microbial consortia at balanced growth', *PLoS ONE*, 2013, **8**, (5), p. e64567
34 Klitgord, N., Segrè, D.: 'Environments that induce synthetic microbial ecosystems', *PLoS Comput. Biol.*, 2010, **6**, (11), p. e1001002
35 Stolyar, S., Van Dien, S., Hillesland, K.L., *et al.*: 'Metabolic modeling of a mutualistic microbial community', *Mol. Syst. Biol.*, 2007, **3**, pp. 92
36 Taffs, R., Aston, J., Brileya, K., *et al.*: 'In silico approaches to study mass and energy flows in microbial consortia: a syntrophic case study', *BMC Syst. Biol.*, 2009, **3**, (1), p. 114
37 Hanly, T.J., Henson, M.A.: 'Dynamic flux balance modeling of microbial co-cultures for efficient batch fermentation of glucose and xylose mixtures', *Biotechnol. Bioeng.*, 2011, **108**, (2), pp. 376–385
38 Salimi, F., Zhuang, K., Mahadevan, R.: 'Genome-scale metabolic modeling of a Clostridial co-culture for consolidated bioprocessing', *Biotechnol. J.*, 2010, **5**, (7), pp. 726–738
39 Zhuang, K., Izallalen, M., Mouser, P., *et al.*: 'Genome-scale dynamic modeling of the competition between *Rhodoferax* and *Geobacter* in anoxic subsurface environments', *ISME J.*, 2011, **5**, (2), pp. 305–316
40 Hanly, T., Urello, M., Henson, M.A.: 'Dynamic flux balance modeling of *S. cerevisiae* and *E. coli* co-cultures for efficient consumption of glucose/xylose mixtures', *Appl. Microbiol. Biotechnol.*, 2012, **93**, (6), pp. 2529–2541
41 Hanly, T.J., Henson, M.A.: 'Dynamic model-based analysis of furfural and HMF detoxification by pure and mixed batch cultures of *S. cerevisiae* and *S. stipitis*', *Biotechnol. Bioeng.*, 2014, **111**, (2), pp. 272–284
42 Hanly, T.J., Henson, M.A.: 'Dynamic metabolic modeling of a microaerobic yeast co-culture: predicting and optimizing ethanol production from glucose/xylose mixtures', *Biotechnol. Biofuels*, 2013, **6**, p. 44
43 Zhuang, K., Ma, E., Lovley, D.R., Mahadevan, R.: 'The design of long-term effective uranium bioremediation strategy using a community metabolic model', *Biotechnol. Bioeng.*, 2012, **109**, (10), pp. 2475–2483
44 Shong, J., Jimenez Diaz, M.R., Collins, C.H.: 'Towards synthetic microbial consortia for bioprocessing', *Curr. Opin. Biotechnol.*, 2012, **23**, (5), pp. 798–802
45 Mahadevan, R., Henson, M.A.: 'Genome-based modeling and design of metabolic interactions in microbial communities', *Comput. Struct. Biotechnol. J.*, 2012, **3**, (4), p. e201210008
46 Henry, C.S., DeJongh, M., Best, A.A., Frybarger, P.M., Linsay, B., Stevens, R.L.: 'High-throughput generation, optimization and analysis of genome-scale metabolic models', *Nat. Biotechnol.*, 2010, **28**, (9), pp. 977–982
47 Karp, P.D., Paley, S.M., Krummenacker, M., *et al.*: 'Pathway Tools version 13.0: integrated software for pathway/genome informatics and systems biology', *Brief Bioinform.*, 2010, **11**, (1), pp. 40–79
48 Feng, X., Xu, Y., Chen, Y., Tang, Y.J.: 'MicrobesFlux: a web platform for drafting metabolic models from the KEGG database', *BMC Syst. Biol.*, 2012, **6**, p. 94
49 Overbeek, R., Begley, T., Butler, R.M., Choudhuri, J.V., Chuang, H.Y., *et al.*: 'The subsystems approach to genome annotation and its use in the project to annotate 1000 genomes', *Nucleic Acids Res.*, 2005, **33**, (17), pp. 5691–5702
50 Förster, J., Famili, I., Fu, P., Palsson, B.Ø., Nielsen, J.: 'Genome-scale reconstruction of the *Saccharomyces cerevisiae* metabolic network', *Genome Res.*, 2003, **13**, (2), pp. 244–253
51 Zomorrodi, A.R., Maranas, C.D.: 'OptCom: a multi-level optimization framework for the metabolic modeling and analysis of microbial communities', *PLoS Comput. Biol.*, 2012, **8**, (2), p. e1002363
52 Varma, A., Palsson, B.Ø.: 'Stoichiometric flux balance models quantitatively predict growth and metabolic by-product secretion in wild-type *Escherichia coli* W3110', *Appl. Environ. Microbiol.*, 1994, **60**, (10), pp. 3724–3731
53 Gadkar, K., DoyleIIIF.J., Edwards, J.S., Mahadevan, R.: 'Estimating optimal profiles of genetic alterations using constraint-based models', *Biotechnol. Bioeng.*, 2005, **89**, (2), pp. 243–251
54 Höffner, K., Harwood, S.M., Barton, P.I.: 'A reliable simulator for dynamic flux balance analysis', *Biotechnol. Bioeng.*, 2013, **110**, (3), pp. 792–802
55 Yomano, L., York, S., Zhou, S., Shanmugam, K., Ingram, L.: 'Re-engineering *Escherichia coli* for ethanol production', *Biotechnol. Lett.*, 2008, **30**, (12), pp. 2097–2103
56 Davison, B.H., Stephanopoulos, G.: 'Coexistence of *S. cerevisiae* and *E. coli* in chemostat under substrate competition and product inhibition', *Biotechnol. Bioeng.*, 1986, **28**, (11), pp. 1742–1752
57 Okuda, N., Ninomiya, K., Katakura, Y., Shioya, S.: 'Strategies for reducing supplemental medium cost in bioethanol production from waste house wood hydrolysate by ethanologenic *Escherichia coli*: inoculum size increase and coculture with *Saccharomyces cerevisiae*', *J. Biosci. Bioeng.*, 2008, **105**, (2), pp. 90–96
58 Qian, M., Tian, S., Li, X., Zhang, J., Pan, Y., Yang, X.: 'Ethanol production from dilute-acid softwood hydrolysate by co-culture', *Appl. Biochem. Biotechol.*, 2006, **134**, (3), pp. 273–283
59 Reed, J., Vo, T., Schilling, C., Palsson, B.O.: 'An expanded genome-scale model of *Escherichia coli* K-12 (iJR904 GSM/GPR)', *Genome Biol.*, 2003, **4**, (9), p. R54
60 Curtis, S.J., Epstein, W.: 'Phosphorylation of D-glucose in *Escherichia coli* mutants defective in glucosephosphotransferase, mannosephosphotransferase and glucokinase', *J. Bacteriol.*, 1975, **122**, (3), pp. 1189–1199
61 Eiteman, M.A., Lee, S.A., Altman, R., Altman, E.: 'A substrate-selective co-fermentation strategy with *Escherichia coli* produces lactate by simultaneously consuming xylose and glucose', *Biotechnol. Bioeng.*, 2009, **102**, (3), pp. 822–827

doi: 10.1049/iet-syb.2013.0021

62 Echave, P., Esparza-Cerón, M.A., Cabiscol, E., Tamarit, J., *et al*.: 'DnaK dependence of mutant ethanol oxidoreductases evolved for aerobic function and protective role of the chaperone against protein oxidative damage in *Escherichia coli*', *Proc. Natl. Acad. Sci.USA*, 2002, **99**, (7), pp. 4626–4631

63 Guijarro, J.M., Lagunas, R.: '*Saccharomyces cerevisiae* does not accumulate ethanol against a concentration gradient', *J. Bacteriol.*, 1984, **160**, (3), pp. 874–878

64 Sonnleitner, B., Käppeli, O.: 'Growth of *Saccharomyces cerevisiae* is controlled by its limited respiratory capacity: Formulation and verification of a hypothesis', *Biotechnol. Bioeng.*, 1986, **28**, (6), pp. 927–937

65 Blank, L.M., Sauer, U.: 'TCA cycle activity in *Saccharomyces cerevisiae* is a function of the environmentally determined specific growth and glucose uptake rates', *Microbiology*, 2004, **150**, (4), pp. 1085–1093

66 Heerde, E., Radler, F.: 'Metabolism of the anaerobic formation of succinic acid by *Saccharomyces cerevisiae*', *Arch. Microbiol.*, 1978, **117**, (3), pp. 269–276

67 Laplace, J.M., Delgenes, J.P., Moletta, R., Navarro, J.M.: 'Alcoholic fermentation of glucose and xylose by *Pichia stipitis*, *Candida shehatae*, *Saccharomyces cerevisiae*, and *Zymomonas mobilis*: oxygen requirement as a key factor', *Appl. Microbiol. Biotechnol.*, 1991, **36**, (2), pp. 158–162

68 Laplace, J.M., Delgenes, J.P., Moletta, R., Navarro, J.M.: 'Ethanol production from glucose and xylose by separated and co-culture processes using high cell density systems', *Process. Biochem.*, 1993, **28**, (8), pp. 519–525

69 Taniguchi, M., Takahiro, I., Tohma, T., Fujii, M.: 'Ethanol production from a mixture of glucose and xylose by co-culture of *Pichia stipitis* and a respiratory-deficient mutant of *Saccharomyces cerevisiae*', *J. Ferment. Bioeng.*, 1997, **83**, (4), pp. 364–370

70 Skoog, K., Hahn-Hägerdal, B.: 'Effect of oxygenation on xylose fermentation by *Pichia stipitis*', *Appl. Environ. Microbiol.*, 1990, **56**, (11), pp. 3389–3394

71 Klinke, H.B., Thomsen, A.B., Ahring, B.K.: 'Inhibition of ethanol-producing yeast and bacteria by degradation products produced during pre-treatment of biomass', *Appl. Microbiol. Biotechnol.*, 2004, **66**, (1), pp. 10–26

72 Liu, Z.L., Moon, J., Andersh, B.J., Slininger, P.J., Weber, S.: 'Multiple gene-mediated NAD(P)H-dependent aldehyde reduction is a mechanism of in situ detoxification of furfural and 5-hydroxymethylfurfural by *Saccharomyces cerevisiae*', *Appl. Microbiol. Biotechnol.*, 2008, **81**, (4), pp. 743–753

73 Petersson, A., Almeida, J.R.M., Modig, T., Karhumaa, K., *et al*.: 'A 5-hydroxymethyl furfural reducing enzyme encoded by the *Saccharomyces cerevisiae* ADH6 gene conveys HMF tolerance', *Yeast*, 2006, **23**, (6), pp. 455–464

74 Taherzadeh, M.J., Gustafsson, L., Niklasson, C., Lidén, G.: 'Physiological effects of 5-hydroxymethylfurfural on *Saccharomyces cerevisiae*', *Appl. Microbiol. Biotechnol.*, 2000, **53**, (6), pp. 701–708

75 Mo, M., Palsson, B., Herrgard, M.: 'Connecting extracellular metabolomic measurements to intracellular flux states in yeast', *BMC Syst. Biol.*, 2009, **3**, (1), p. 37

76 Heer, D., Heine, D., Sauer, U.: 'Resistance of *Saccharomyces cerevisiae* to high concentrations of furfural is based on NADPH-dependent reduction by at least two oxireductases', *Appl. Environ. Microbiol.*, 2009, **75**, (24), pp. 7631–7638

77 Almeida, J.M., Bertilsson, M., Hahn-Hägerdal, B., Lidén, G., Gorwa-Grauslund, M.-F.: 'Carbon fluxes of xylose-consuming *Saccharomyces cerevisiae* strains are affected differently by NADH and NADPH usage in HMF reduction', *Appl. Microbiol. Biotechnol.*, 2009, **84**, (4), pp. 751–761

78 Slininger, P.J., Thompson, S.R., Weber, S., Liu, Z.L., Moon, J.: 'Repression of xylose-specific enzymes by ethanol in *Scheffersomyces* (*Pichia*) *stipitis* and utility of repitching xylose-grown populations to eliminate diauxic lag', *Biotechnol. Bioeng.*, 2011, **108**, (8), pp. 1801–1815

79 Jones, R.P.: 'Biological principles for the effects of ethanol', *Enzyme Microb. Technol.*, 1989, **11**, (3), pp. 130–153

80 Lohmeier-Vogel, E.M., Sopher, C.R., Lee, H.: 'Intracellular acidification as a mechanism for the inhibition by acid hydrolysis-derived inhibitors of xylose fermentation by yeasts', *J. Ind. Microbiol. Biotechnol.*, 1998, **20**, (2), pp. 75–81

81 Schneider, H.: 'Selective removal of acetic acid from hardwood-spent sulfite liquor using a mutant yeast', *Enzyme Microb. Technol.*, 1996, **19**, (2), pp. 94–98

82 Weuster-Botz, D.: 'Parallel reactor systems for the bioprocess development', in Scheper, T. (Ed.): 'Advances in biochemical engineering/biotechnology' (Springer-Verlag, 2004), pp. 125–143

83 Abubucker, S., Segata, N., Goll, J., Schubert, A.M., Izard, J., *et al*.: 'Metabolic reconstruction for metagenomic data and its application to the human microbiome', *PLoS Comput. Biol.*, 2012, **8**, p. e1002358